

**A Production in  $e^+e^-$  Annihilations at 29 GeV**

S. Abachi, P. Baringer, I. Beltrami,<sup>(a)</sup> B.G. Bylsma, R. DeBonte, D. Koltick,  
F.J. Loeffler, E.H. Low, R.L. McIlwain, D.H. Miller, C.R. Ng,  
L.K. Rangan<sup>(b)</sup> and E.I. Shibata  
*Purdue University, W. Lafayette, IN 47907*

M. Derrick, K.K. Gan,<sup>(c)</sup> P. Kooijman, J.S. Loos, B. Musgrave,  
L.E. Price, J. Repond, J. Schlereth, K. Sugano, J.M. Weiss<sup>(d)</sup> and D.E. Wood<sup>(b)</sup>  
*Argonne National Laboratory, Argonne, IL 60439*

D. Blockus, B. Brabson, J.M. Brom, J.-P. Guillaud,<sup>(e)</sup> S.W. Gray,<sup>(f)</sup>  
C. Jung, H. Neal,<sup>(g)</sup> H. Ogren, D.R. Rust and M. Valdata-Nappi<sup>(h)</sup>  
*Indiana University, Bloomington, IN 47405*

C. Akerlof, G. Bonvicini, J. Chapman, D. Errede, N. Harnew,<sup>(i)</sup> P. Kesten,<sup>(j)</sup>  
D.I. Meyer, D. Nitz, A.A. Seidl,<sup>(c)</sup> R. Thun, T. Trinko<sup>(c)</sup> and M. Willutzky  
*University of Michigan, Ann Arbor, MI 48109*

B. Cork

*Lawrence Berkeley Laboratory, Berkeley, CA 94720*

This paper presents measurements of the inclusive production cross sections of  $\Lambda$  baryons in  $e^+e^-$  annihilations at  $\sqrt{s} = 29$  GeV. The data sample corresponds to an integrated luminosity of  $256 \text{ pb}^{-1}$  collected with the High Resolution Spectrometer at PEP. Comparisons are made to the predictions of the Lund model. The data are well described using a strange diquark suppression parameter,  $(us/ud)/(s/d)$ , of  $0.89 \pm 0.10^{+0.56}_{-0.16}$ , and the measured  $\Lambda_c \rightarrow \Lambda + X$  branching ratio of  $23 \pm 10\%$ . No polarization is observed in the  $\Lambda$  decays.

(Submitted by P. Baringer to the XXIII International Conference  
on High Energy Physics, Berkeley, California)

## 1. INTRODUCTION

The inclusive cross sections for lambda ( $\Lambda$ ) production in high energy  $e^+e^-$  annihilations into hadrons have been measured by several experiments.<sup>1-4</sup> In this paper we present new results on  $\Lambda$  production from a large sample of data collected over a period of four years with the High Resolution Spectrometer (HRS) at the PEP  $e^+e^-$  storage ring. The data, taken from an integrated luminosity of  $256 \pm 8 \text{ pb}^{-1}$  at  $\sqrt{s} = 29 \text{ GeV}$ , are compared to predictions of the Lund model<sup>5</sup> for the inclusive  $\Lambda$  differential cross sections as a function of fractional energy,  $z = 2E_\Lambda/\sqrt{s}$ , and rapidity,  $y = \frac{1}{2} \ln[(E_\Lambda + p_\parallel)/(E_\Lambda - p_\parallel)]$ . Measurements of the polarization of the  $\Lambda$  are also made, and  $\Lambda - \bar{\Lambda}$  correlations are examined.

In the Lund string model, baryons are produced when a quark and a diquark (members of neighboring pairs produced from the vacuum) are joined by a strong force flux tube of sufficient energy. The production rate of baryons relative to mesons in the fragmentation chain is controlled, in this model, by a parameter that gives the relative probability of forming a diquark pair versus a quark pair. Physically, the diquark is pictured as an object of mass  $m$  that couples to the color field as a unit. The suppression of diquarks (and of heavy quarks) arises from a tunneling probability that is proportional to  $\exp(-m^2/K^2)$ , where  $K \approx 250 \text{ MeV}$ . The production of a  $\Lambda$  is suppressed both because it is a baryon and because it contains a strange quark. The strangeness may come either from the quark or from the diquark. The ratio of strange quark production to light quark production,  $s/u$ , is a parameter of the model. Any additional suppression of strangeness in diquarks is specified by the parameter  $\delta = (us/ud)/(s/d)$ .

A second important source of  $\Lambda$  hyperons is the decay of charmed baryons.

The shapes of the  $z$  and  $y$  differential cross sections are different for  $\Lambda$  hyperons coming from these two sources, and so their relative contributions can, in principle, be measured given sufficiently precise data.

The  $\Lambda$  particle is readily identifiable via its long-lived decay to  $p\pi$ . At PEP energies, the  $\Lambda$  and  $\bar{\Lambda}$  are easily distinguished from one another because the proton (antiproton) must carry more momentum than the pion in the lab frame whenever the parent  $\Lambda$  ( $\bar{\Lambda}$ ) has  $z > 0.08$ . Throughout the following discussion we will use ' $\Lambda$ ' to refer to both the lambda baryon and its antiparticle, and cross sections given for the ' $\Lambda$ ' will be the sums of the  $\Lambda$  and  $\bar{\Lambda}$  values.

## 2. DETECTOR AND $\Lambda$ SELECTION

Features of the HRS detector<sup>6</sup> relevant to the present analysis include a fifteen layer central drift chamber, with tracking layers spanning the radial distances from 21 to 103 cm, and covering 90% of  $4\pi$  in solid angle, and a two layer outer drift chamber system at a radius of 190 cm, which covers 65% of  $4\pi$ . Both chamber systems are contained within the 16.2 kG solenoidal magnetic field. The momentum resolution for tracks which pass through the outer drift chamber layers is  $\sigma_p = 2 \times 10^{-3} p^2$  (GeV/c).

The hadronic data sample was selected by a series of simple cuts,<sup>7</sup> which included the requirements of at least four charged tracks and a scalar sum of the momenta greater than 5.8 GeV/c. Events containing less than 7.0 GeV of charged particle energy were required to have a total energy (including the energy in the electromagnetic shower counters) of at least 8.0 GeV.

The decays  $\Lambda \rightarrow p\pi^-$  were identified through a series of cuts that favored

neutral track pairs coming from secondary decay vertices. The principal requirements were:

- Each track had to be well reconstructed, using at least 60% of the drift chamber cells traversed.
- For each pair of tracks, the one with the lower momentum was assumed to be the pion, and was required to miss the primary event vertex by at least 0.2 cm in the plane perpendicular to the beam direction.
- The two decay tracks were required to intersect in that transverse plane at a radial distance of between 1.5 and 75.0 cm, and to pass within 2 cm of each other along the beam direction at this intersection point.
- The reconstructed neutral momentum vector, when projected through the secondary vertex point, was required to come within 0.3 cm of the primary event vertex.
- Vee candidates satisfying the above criteria were fitted to a three-dimensional secondary vertex. The  $\chi^2$  of this fit was required to be less than 10.
- Vee candidates having an invariant mass within 10 MeV of the  $K^0$  mass, when both tracks are interpreted as pions, were rejected.

These cuts produce an exceptionally narrow peak in the  $p\pi$  mass spectrum, as shown in Fig. 1. The spatial resolution of the tracking chambers, and the small amount of material between the beam crossing point and the central drift chamber, combined with the high magnetic field, allow the extraction of a  $\Lambda$  sample with a good signal to noise ratio across a range of fractional energies that extends to  $z = 0.8$ . The signal in the high  $z$  region is shown separately in Fig. 1(b).

The background distributions were determined from the data by reflecting the reconstructed momentum vector of all negatively charged tracks through the origin, and applying the same vee finding analysis. These background vees produce a  $p - \pi$  mass spectrum whose shape agrees with that of the data in the region away from the  $\Lambda$  mass peak. The distribution was normalized to give the proper number of events in the wings and subtracted from the data. The signal in Fig. 1(a) contains  $1514 \pm 85$   $\Lambda$  and  $1407 \pm 85$   $\bar{\Lambda}$  events. Using Breit-Wigner forms to fit the peak regions,<sup>9</sup> we obtain central mass values of  $1115.7 \pm 0.1$  MeV for the  $\Lambda$  and  $1115.6 \pm 0.1$  MeV for the  $\bar{\Lambda}$ , in good agreement with world average values.<sup>9</sup> The widths ( $\Gamma$ ) are found to be  $5.0 \pm 0.3$  MeV for the  $\Lambda$  and  $4.9 \pm 0.3$  MeV for the  $\bar{\Lambda}$ , in excellent agreement with Monte Carlo studies of the detector resolution. In determination of the inclusive distributions below, the  $\Lambda$  signal was selected in the mass region between 1110.6 and 1120.6 MeV.

### 3. SCALING CROSS SECTION AND RAPIDITY DISTRIBUTION

The detector acceptance was calculated as a function of  $z$ , using hadronic events simulated by a Monte Carlo program. The acceptance function peaks at  $z = 0.25$ , where 13% of  $\Lambda \rightarrow p\pi^-$  decays are reconstructed; the overall acceptance for  $\Lambda \rightarrow p\pi^-$  is 7.5%. The scaling cross section  $s/\beta \cdot d\sigma/dz$ , also corrected for the known branching ratio into  $p\pi^-$ ,<sup>9</sup> is shown in Fig. 2 as a function of the fractional energy variable  $z$ . The statistical and systematic errors, which are given separately in Table 1, have been summed in quadrature in Fig. 2. The systematic uncertainties include the background subtraction, acceptance correction, and luminosity determination. The results are in good agreement with

earlier experiments<sup>1-3</sup> in the region of overlap. The HRS data at high  $z$  indicate a continuation of the previously observed exponential fall in the scaling cross section.

The  $\Lambda$  rapidity was calculated relative to a thrust axis, which was determined for each event using all well-measured charged tracks. Tracks tagged as coming from a  $K^0$  or  $\Lambda$  decay were included in the thrust calculation as a single neutral track, constrained to a secondary vertex. Events in which the thrust axis was not well-contained within the tracking volume were rejected from the data sample. The acceptance corrected rapidity distribution is shown in Fig. 3 and listed in Table 2.

#### 4. POLARIZATIONS

The distribution of the angle of the proton (antiproton) in the center-of-mass of the  $\Lambda$  ( $\bar{\Lambda}$ ) was examined for evidence of polarizations of the  $\Lambda$  ( $\bar{\Lambda}$ ) spin direction. One such polarization is expected along the direction of flight ( $l$ ) of the  $\Lambda$  due to the  $\gamma - Z^0$  interference term in the  $e^+e^- \rightarrow q\bar{q}$  process. This polarization varies with the lab production angle ( $\theta$ ) of the initial quark. Non-leading  $\Lambda$  particles would not be polarized by this mechanism. The polarization  $P$  is related to the forward-backward asymmetry ( $A$ ) of the proton direction along the chosen axis by  $A = 0.5\alpha P$ , where  $\alpha$  is the weak decay parameter of the  $\Lambda$ . Asymmetries were calculated separately for  $\Lambda$  and  $\bar{\Lambda}$  and in various  $z$  and  $\cos\theta$  bins. The asymmetries were all consistent with zero within statistical errors. The asymmetry for the total data sample ( $\Lambda$  and  $\bar{\Lambda}$  summed) is  $A = 0.037 \pm 0.043$ . With the cut  $z \geq 0.3$ , the result is  $A = -0.13 \pm 0.09$ . A correction has

been applied to the data because the acceptance for  $A$  particles with a backward directed proton is much higher than for those with a forward directed proton. The above errors include both the statistical errors in the data, and the uncertainty in the acceptance corrections.

A second possible source of polarization has been discussed by the Lund group<sup>5</sup>. In their string picture, the massive baryon and antibaryon must be separated along the color flux direction ( $C$ ). The transverse momenta of the baryons produce a net angular momentum which must be compensated by aligning the spins of the particles in the direction ( $C \times I$ ). The resulting polarization scales as the transverse momentum divided by the beam energy. Experimentally, it is difficult to determine  $C$ . For two-jet like events the thrust axis approximates the initial quark direction. Using a rapidity weighted dipole formula,  $D = \Sigma y \cdot Q / \Sigma |y|$  where the sums are over all charged tracks in the event and  $Q$  is the charge, one can determine the direction of the positively charged parton.<sup>10</sup> Monte Carlo calculations indicate that for events satisfying the sphericity and aplanarity cuts,  $S \leq 0.25$  and  $A \leq 0.15$ , the quark direction is correctly identified by this technique in 63% of the events. (At PEP energies eight out of eleven, or about 73%, of the hadronic events come from a charge  $+\frac{2}{3}$  quark.) Using these two-jet selection cuts, the asymmetry along the ( $C \times I$ ) axis was measured for three different ranges of the  $A$   $p_T^2$ . The values obtained were:  $A = 0.04 \pm 0.06$  for  $p_T^2 \leq 0.4$ ,  $A = 0.05 \pm 0.08$  for  $0.4 \leq p_T^2 \leq 1.0$ , and  $A = -0.01 \pm 0.08$  for  $p_T^2 \geq 1.0$ . Quoted errors are statistical only. The uncertainty in the calculation of the color flow tagging efficiency adds a systematic error of  $\pm 0.03$  to each of the asymmetry values.

## 5. DETERMINATION OF $\delta$

In order to determine the value of the strange diquark suppression parameter  $\delta$ , the  $z$  and  $y$  distributions were fitted to the predictions of the Lund model varying  $\delta$  from 0 to 1.5. The other important parameters of the model were set to the values  $s/u = 0.34 \pm 0.03$ , as determined from the ERS data on  $K^0$ ,  $K^{*0}$  and  $\phi$  production,<sup>11</sup> and  $qq/q = 0.078 \pm 0.005$ , as determined from the baryon data of the TPC group.<sup>12</sup> The inclusive branching ratio ( $\mathbf{B}$ ) for  $\Lambda_c \rightarrow \Lambda + X$  was fixed to the value  $\mathbf{B} = 23 \pm 10\%$ , as reported by the SLAC Hybrid Facility Photon Collaboration.<sup>13</sup> Fitting both the  $z$  and the  $y$  distributions, we obtain  $\delta = 0.89 \pm 0.10$ . These parameters give the solid curves in Figs. 2 and 3, both of which agree well with the data. The contributions from charmed baryon decay alone are shown by the dot-dashed lines in Figs. 2 and 3. These distributions peak near  $z = 0.3$  and  $y = 2.0$ , in contrast to the  $\Lambda$  particles coming from the fragmentation chain which populate the regions at low  $z$  and low rapidity.

The statistical and the systematic uncertainties in the data were both included in the  $\chi^2$  calculations and are reflected in the error of  $\pm 0.10$  on  $\delta$ . This error, however, does not reflect the uncertainties in the other Lund parameters,  $qq/q$  and  $s/u$ , or in  $\mathbf{B}$ . In order to reproduce the total inclusive cross section of the  $\Lambda$ , these parameters must satisfy the approximate relation:

$$\frac{qq}{q} \cdot \frac{s}{u} (1 + \delta) + C_1 \mathbf{B} = \text{const.},$$

where  $C_1$  is a constant proportional to the total production rate for charmed baryons. This production rate has not been directly measured at PEP energies,



and for this analysis it is taken to be  $2 \cdot \frac{\delta}{\Pi} \cdot qq/q$  charmed baryons per hadronic event. This is a reasonable but unsubstantiated assumption. Thus, although  $\mathbf{B}$  is discussed as the parameter in question, one can regard the product  $C_1\mathbf{B}$  as the true unknown.

Fig. 4 shows the variation of  $\delta$  with  $\mathbf{B}$ , as determined from  $\chi^2$  fits to the  $z$  and  $y$  distributions of the  $\Lambda$ . The dashed lines represent the  $1\sigma$  errors in  $\delta$  for fixed  $\mathbf{B}$ . The shapes of both the  $z$  and  $y$  distributions are best described with no contribution from charmed baryon decay. The  $\chi^2$  of the fit steadily increases as one follows the band of best values from  $\mathbf{B} = 0\%$  to  $\mathbf{B} = 50\%$ . If the experimental measurement of  $\mathbf{B}^{13}$  is included as a constraint in the fit, then the  $1\sigma$  upper and lower bounds on  $\delta$  are 1.45 and 0.80. Based on these considerations, and on the quoted uncertainties in  $qq/q$  and  $s/u$ , we assign an additional systematic error of  $^{+0.56}_{-0.16}$  to the  $\delta$  measurement.

As a further check, we note that the set of Lund parameters reported here imply a production of 0.024  $\Xi^-$  particles per event, in good agreement with the measurements of  $0.026 \pm 0.012$   $\Xi^-$ 's per event by the TASSO group,<sup>14</sup> and  $0.020 \pm 0.009$   $\Xi^-$ 's per event by the TPC group.<sup>12</sup> A determination from these  $\Xi^-$  numbers alone yields  $\delta = 0.88 \pm 0.39$ .

## 6. EVENTS WITH $\Lambda$ and $\bar{\Lambda}$

An evaluation of  $\delta$  can also be made from the cross section for events containing both a  $\Lambda$  and  $\bar{\Lambda}$ . There are 21 such events in the present data sample, with an estimated background of  $3.3 \pm 2.1$  events, giving a mean multiplicity of  $\langle n_{\Lambda-\bar{\Lambda}} \rangle = 0.054 \pm 0.014 \pm 0.012$  pairs per hadronic event. The first error is

statistical, the second systematic. This value, averaged with the TPC<sup>2</sup> measurement of  $\langle n_{\Lambda-\bar{\Lambda}} \rangle = 0.042 \pm 0.017 \pm 0.014$  and compared with the Lund model prediction for  $\langle n_{\Lambda-\bar{\Lambda}} \rangle$ , leads to a value of  $\delta = 0.77 \pm 0.35$ . Both this measurement and the  $\Xi^-$  production measurement are in reasonable agreement with our previous result, but neither is precise enough to rule out the low  $\delta$  region.

Fig. 5a. shows the angular separation  $\theta$  between the  $\Lambda$  and the  $\bar{\Lambda}$  in the 21 events. Events accumulate near  $\cos\theta$  of -1 and 1 due to the two-jet structure of the events, but the excess of events near  $\cos\theta = 1$  indicates that the baryon number of the  $\Lambda$  is preferentially compensated within the same jet. An underlying random distribution of events is expected both from background events and because the  $\Lambda$  and  $\bar{\Lambda}$  may come from different baryon-antibaryon pairs in the fragmentation chain. The rapidity difference  $\Delta y$ , shown in Fig. 5b., shows the same effect of local baryon number conservation on top of a random distribution. Both plots agree well with the predictions of the Lund model which features local baryon number conservation. The total number of observed  $\Lambda - \bar{\Lambda}$  events indicates that the baryon number and strangeness of the  $\Lambda$  are compensated by a  $\bar{\Lambda}$  (or by an antibaryon which decays into a  $\bar{\Lambda}$ ) roughly half of the time.

If baryon number is always compensated by an antibaryon which is neighboring in rank, then one might expect the momenta of the baryon and antibaryon to be equal and opposite in the plane transverse to the thrust axis.<sup>15</sup> This effect would be diluted in the data due to gluon radiation (the two-jet selection cuts have not been applied here) and the above mentioned random background. The angular separation  $\Delta\phi$  in the plane transverse to the thrust axis is plotted in Fig. 5c. No evidence for any correlation is seen in the data. If mesons are

produced between the baryon and antibaryon in the fragmentation chain, as in the Lund "popcorn" model,<sup>16</sup> the  $p_T$  correlations are weakened further. The Lund prediction, with their parameter  $P(BM\bar{B})/(P(B\bar{B}) + P(BM\bar{B})) = 0.5$  gives reasonable agreement with the data. Lack of statistics prevents making any meaningful measurement of this "popcorn" parameter, however.

## 7. TOTAL CROSS SECTION AND CONCLUSIONS

In quoting a total  $\Lambda$  production cross section, it is important to specify the correction made for the unobserved momentum region. In the range from  $z = 0.1$  to 0.8, where a good signal is obtained, the ratio to the  $\mu$ -pair point cross section is measured to be  $R_\Lambda = 0.678 \pm 0.023 \pm 0.047$ . Using the solid curve of Fig. 2, the correction is 20.9%, which results in a total multiplicity of  $\langle n_\Lambda \rangle = 0.220 \pm 0.007 \pm 0.022$  per event.<sup>17</sup>

In summary, the fits of the Lund model to the inclusive  $\Lambda$  data presented here show that very little extra suppression of the strange flavor is needed in diquark pair production over that already found for single quark pair production. Previous analyses of inclusive  $\Lambda$  data have reported values for the Lund strange diquark suppression parameter,  $\delta$ , of 0.32<sup>1</sup> and 0.2.<sup>2</sup> These values were obtained with a version of the Lund Monte Carlo procedure<sup>5</sup> which yields a value of 50% for the inclusive branching ratio  $\Lambda_c \rightarrow \Lambda + X$ . Substantially better agreement with the present data is achieved, when the experimentally measured value of  $B = 23 \pm 10\%$  is used, and a value  $\delta = 0.89 \pm 0.10_{-0.16}^{+0.56}$  is obtained. No polarization is observed in the  $\Lambda$  decays, either along the direction of flight of the  $\Lambda$  ( $l$ ), or along the  $(C \times l)$  axis where  $C$  is the color flow direction. The 21 events in

which both a  $\Lambda$  and  $\bar{\Lambda}$  were reconstructed show evidence of local baryon number conservation, but no correlation in the momentum components transverse to the thrust axis.

We would like to express our gratitude to the technical staffs of PEP, and of the collaborating institutions, without whom this experiment would not have been possible. This work was supported in part by the U.S. Department of Energy under Contracts W-31-109-Eng-38, DE-AC02-76ER01112, DE-AC03-76SF00098, DE-AC02-76ER01428, and DE-AC02-84ER40125. The work of H. Neal, M. Daigo, and M. Valdata-Nappi was supported in part by the State University of New York at Stony Brook. H. Neal also received support from the J. S. Guggenheim Foundation.

#### DISCLAIMER

This report was prepared as an account of work sponsored by an agency of the United States Government. Neither the United States Government nor any agency thereof, nor any of their employees, makes any warranty, express or implied, or assumes any legal liability or responsibility for the accuracy, completeness, or usefulness of any information, apparatus, product, or process disclosed, or represents that its use would not infringe privately owned rights. Reference herein to any specific commercial product, process, or service by trade name, trademark, manufacturer, or otherwise does not necessarily constitute or imply its endorsement, recommendation, or favoring by the United States Government or any agency thereof. The views and opinions of authors expressed herein do not necessarily state or reflect those of the United States Government or any agency thereof.

- (a) Present address: ETH, Zurich, Switzerland.
- (b) Present address: Lockheed Missiles and Space Co., Sunnyvale, CA 94086.
- (c) Present address: Stanford Linear Accelerator Center, Stanford, CA 94305.
- (d) Present address: SRI international, Menlo Park, CA 94025.
- (e) Present address: LAPP, Annecy-le-Vieux, France.
- (f) Present address: Laboratory of Nuclear Studies, Cornell University, Ithaca, NY 14853.
- (g) Present address: Department of Physics, State University of New York at Stony Brook, Stony Brook, NY 11794.
- (h) On leave from INFN, Pisa, Italy.
- (i) Present address: CERN, 1211 Geneva 23, Switzerland.
- (j) Present address: Brandeis University, Waltham, MA 02254.

## REFERENCES

1. TASSO collaboration, R. Brandelik *et al.*, *Phys. Lett.* 105B, 75 (1981);  
M. Althoff *et al.*, *Z. Phys.* C27, 27 (1985).
2. TPC collaboration, H. Aihara *et al.*, *Phys. Rev. Lett.* 54, 274 (1985).
3. MARK II collaboration, C. de la Vaissiere *et al.*, *Phys. Rev. Lett.* 54,  
2071 (1985).
4. CLEO collaboration, M.S. Alam, *et al.*, *Phys. Rev. Lett.* 53, 24 (1984);  
S. Behrends *et al.*, *Phys. Rev. D*31, 2161 (1985).
5. B. Andersson, G. Gustafson and T. Sjostrand, *Nucl. Phys.* B197, 45  
(1982); *Phys. Rep.* 97, 32 (1983). Version 5.3 of the Lund Monte Carlo  
was used in this analysis.
6. A more complete description of the apparatus can be found in: D. Bender  
*et al.*, *Phys. Rev. D*30, 515 (1984).
7. D. Bender *et al.*, *Phys. Rev. D*31, 1 (1985).
8. The detector resolution function, when integrated over the broad momen-  
tum range of the data sample, is well approximated by the Breit-Wigner  
form.
9. Particle Data Group, *Rev. Mod. Phys.* 56, 1 (1984).
10. This method was developed by the TPC group. H. Yamamoto, private  
communication.
11. M. Derrick *et al.*, *Phys. Lett.* 153B, 519 (1985); *Phys. Rev. Lett.* 54,  
2568 (1985).

12. H. Yamamoto, in *QCD and Beyond, Proceedings of the Twentieth Rencontres de Moriond, 1985*, edited by J. Tran Thanh Van (Editions Frontieres, Gif-sur-Yvette, France, 1985), p. 91.
13. K. Abe *et al.*, *Phys. Rev. D* **33**, 1 (1986).
14. TASSO collaboration, M. Althoff *et al.*, *Phys. Lett.* **130B**, 340 (1983).
15. A. Bartl, *Phys. Lett.* **122B**, 427 (1983).
16. B. Andersson, G. Gustafson and T. Sjostrand, LU TP 84-9 (1984).
17. Using the Lund curve with  $\delta = 0.3$  and  $B = 50\%$  to extrapolate to  $z = 0$  and  $z = 1$  gives an 18.3% correction, and a total multiplicity of  $\langle n_{\Delta} \rangle = 0.214 \pm 0.007 \pm 0.021$ . This number agrees well with the values reported by the Mark II and TPC collaborations.

## FIGURE CAPTIONS

1. Invariant mass spectra resulting from oppositely charged track pairs satisfying the cuts described in text for a) all  $z$ , and b)  $0.4 < z < 0.8$ . The higher momentum track of the pair is interpreted as  $p(\bar{p})$ , the lower as  $\pi^-(\pi^+)$ .
2. Measurements of the scaling cross section,  $s/\beta \cdot d\sigma/dz$ , for inclusive  $\Lambda$  production. Data from the Mark II, TPC, and TASSO detectors are shown for comparison. The solid curve is given by the Lund Monte Carlo, with  $\delta = 0.89$  and a branching ratio for  $\Lambda_c \rightarrow \Lambda + X$  of 23%. The dot-dashed curve represents the contribution from charmed baryon decay.
3. The rapidity distribution,  $1/\sigma \cdot d\sigma/dy$ , for inclusive  $\Lambda$  production, where  $y$  is measured relative to the thrust axis. The solid curve is given by the Lund Monte Carlo, with  $\delta = 0.89$  and  $BR(\Lambda_c \rightarrow \Lambda + X) = 23\%$ . The dot-dashed curve represents the contribution from charmed baryon decay ( $\times 10$ ).
4. Best fit values of the Lund strange diquark suppression parameter  $\delta$  as a function of the assumed inclusive branching ratio ( $B$ ) for  $\Lambda_c \rightarrow \Lambda + X$ . The dashed lines represent  $1\sigma$  errors in  $\delta$  for fixed  $B$ .
5. Events containing both a  $\Lambda$  and  $\bar{\Lambda}$ . (a) shows the angle  $\theta$  between the two particles, (b) the rapidity gap, and (c) the angular separation  $\Delta\phi$  in the plane transverse to the thrust axis.



$s$	$(\sigma/\beta)(d\sigma/dz)(nb \cdot GeV^2)$
0.100-0.125	1053±95±269
0.125-0.150	514.0±47.0±68.6
0.150-0.175	355.2±33.4±47.0
0.175-0.200	307.4±28.0±40.3
0.200-0.225	198.7±23.0±22.2
0.225-0.275	150.3±13.4±16.6
0.275-0.325	86.0±10.1±10.7
0.325-0.375	52.5±8.7±7.9
0.375-0.425	51.2±7.8±7.9
0.425-0.500	28.8±5.2±5.7
0.500-0.600	11.1±2.7±2.6
0.600-0.800	2.00±1.09±0.47

Table 1. Lambda Invariant Cross Section vs.  $z$

$y$	$(1/\sigma)(d\sigma/dy)$
0.2-0.5	0.243±0.029±0.079
0.5-0.8	0.115±0.015±0.027
0.8-1.0	0.148±0.013±0.029
1.0-1.2	0.124±0.011±0.017
1.2-1.4	0.108±0.009±0.020
1.4-1.7	0.0834±0.0069±0.0110
1.7-2.0	0.0535±0.0055±0.0065
2.0-2.3	0.0472±0.0054±0.0081
2.3-2.6	0.0192±0.0040±0.0057
2.6-3.2	0.0060±0.0021±0.0016

Table 2. Lambda Invariant Cross Section vs.  $y$

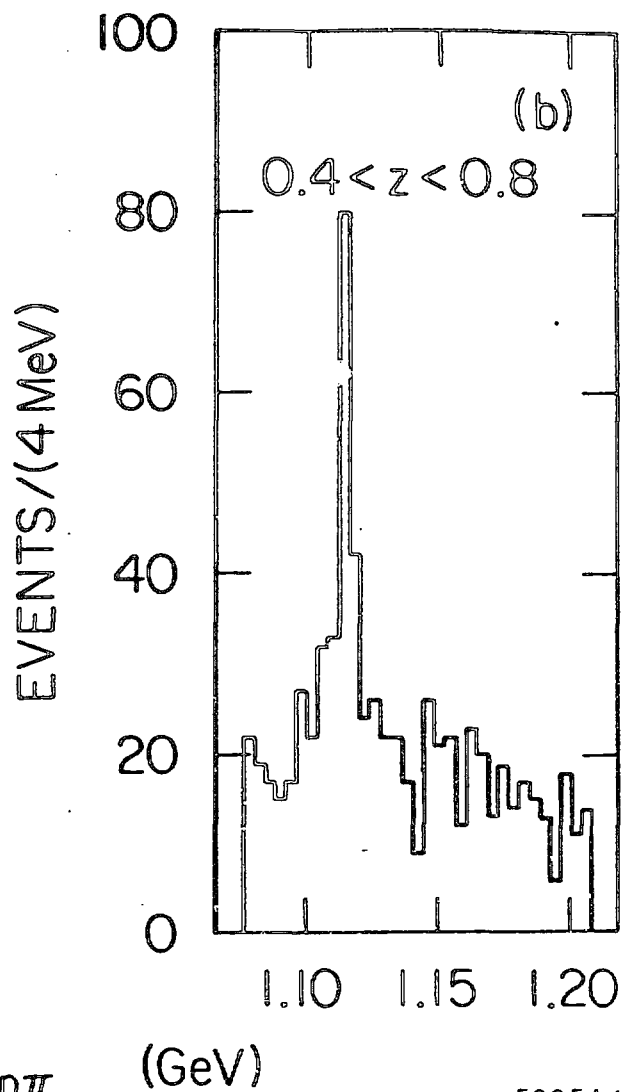
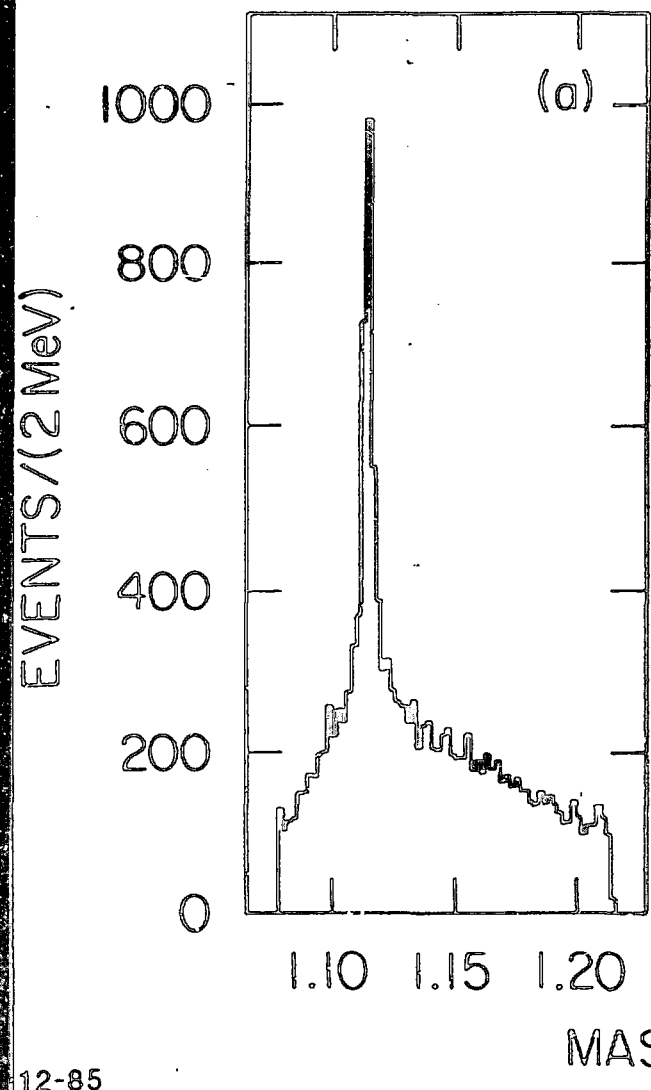


Fig. 1

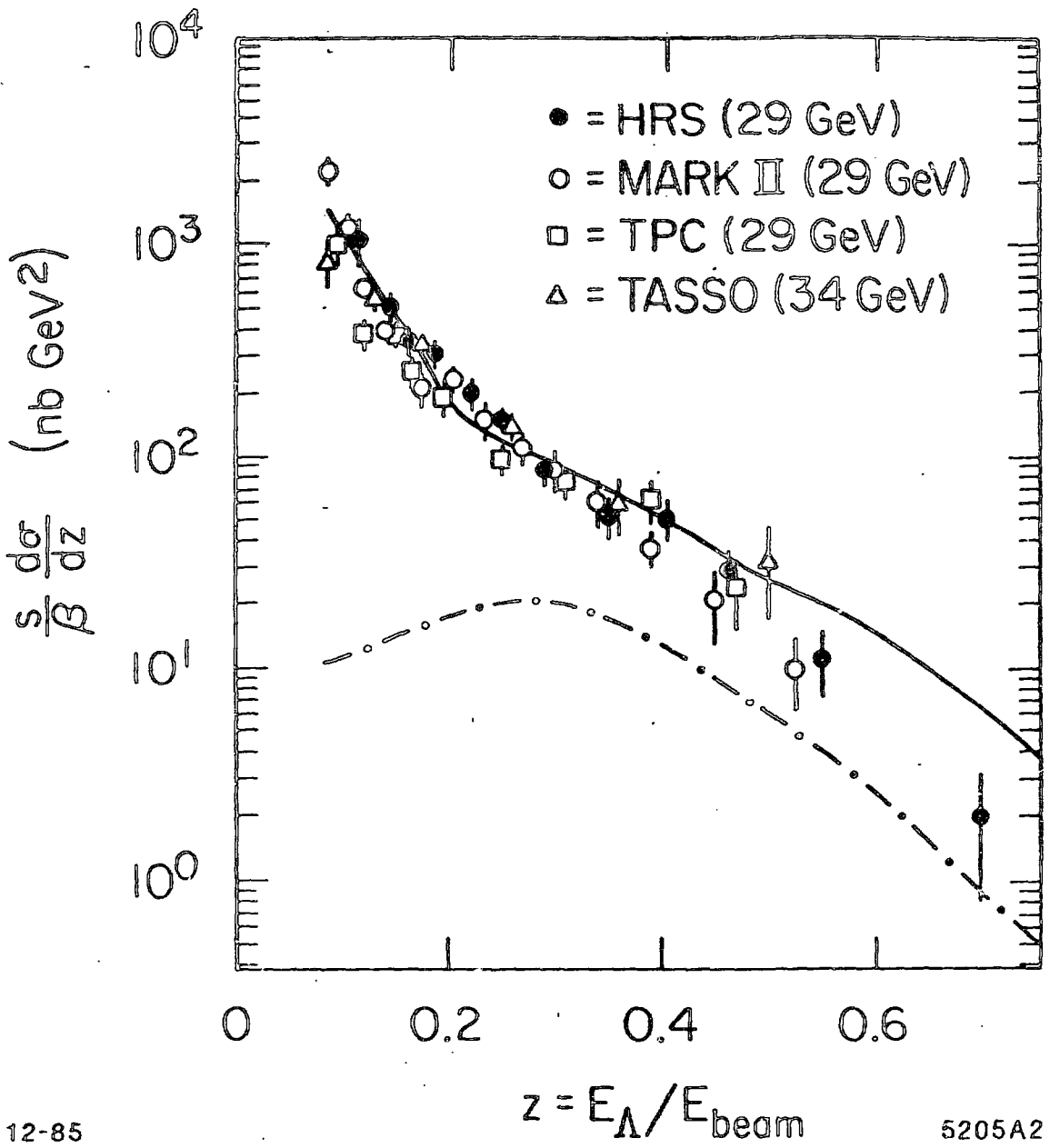
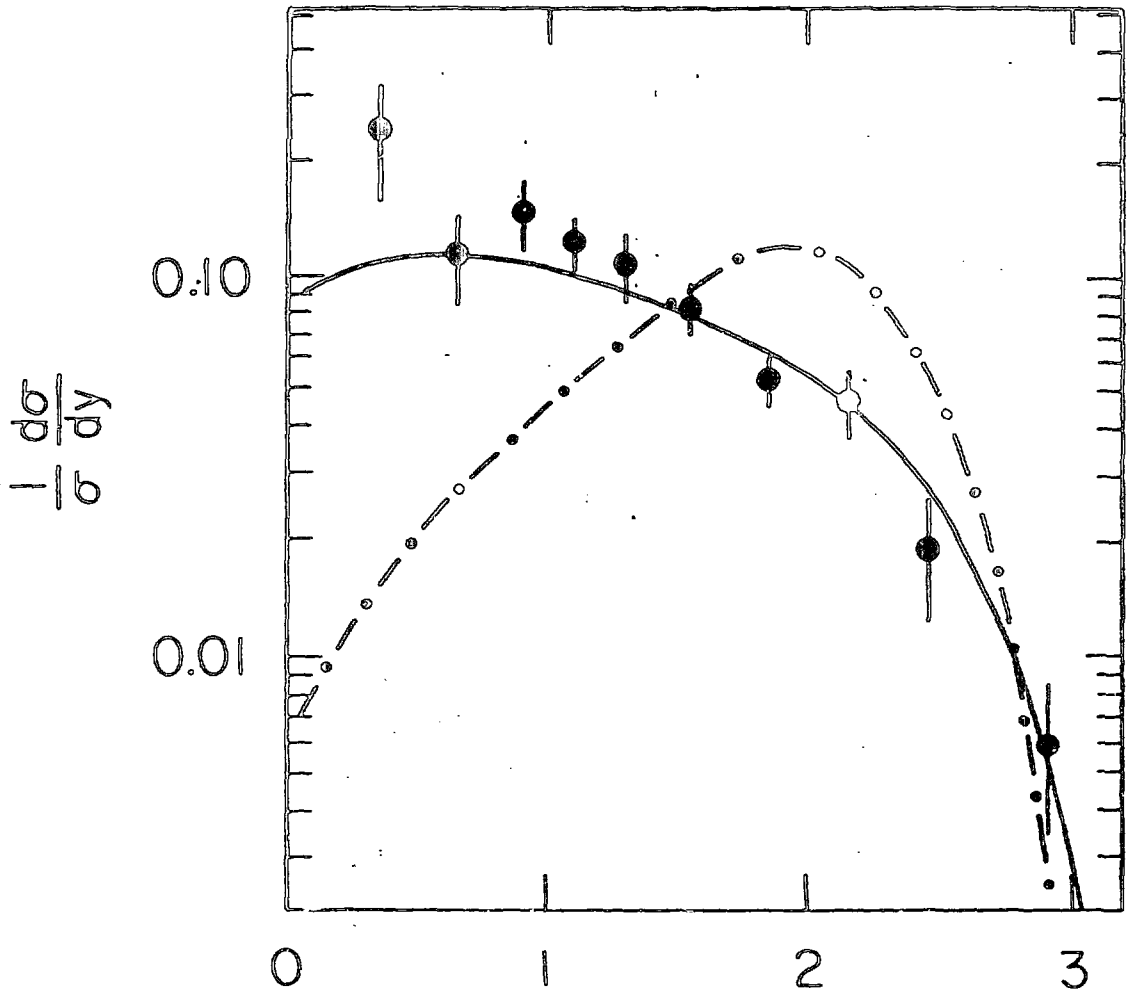


Fig. 2

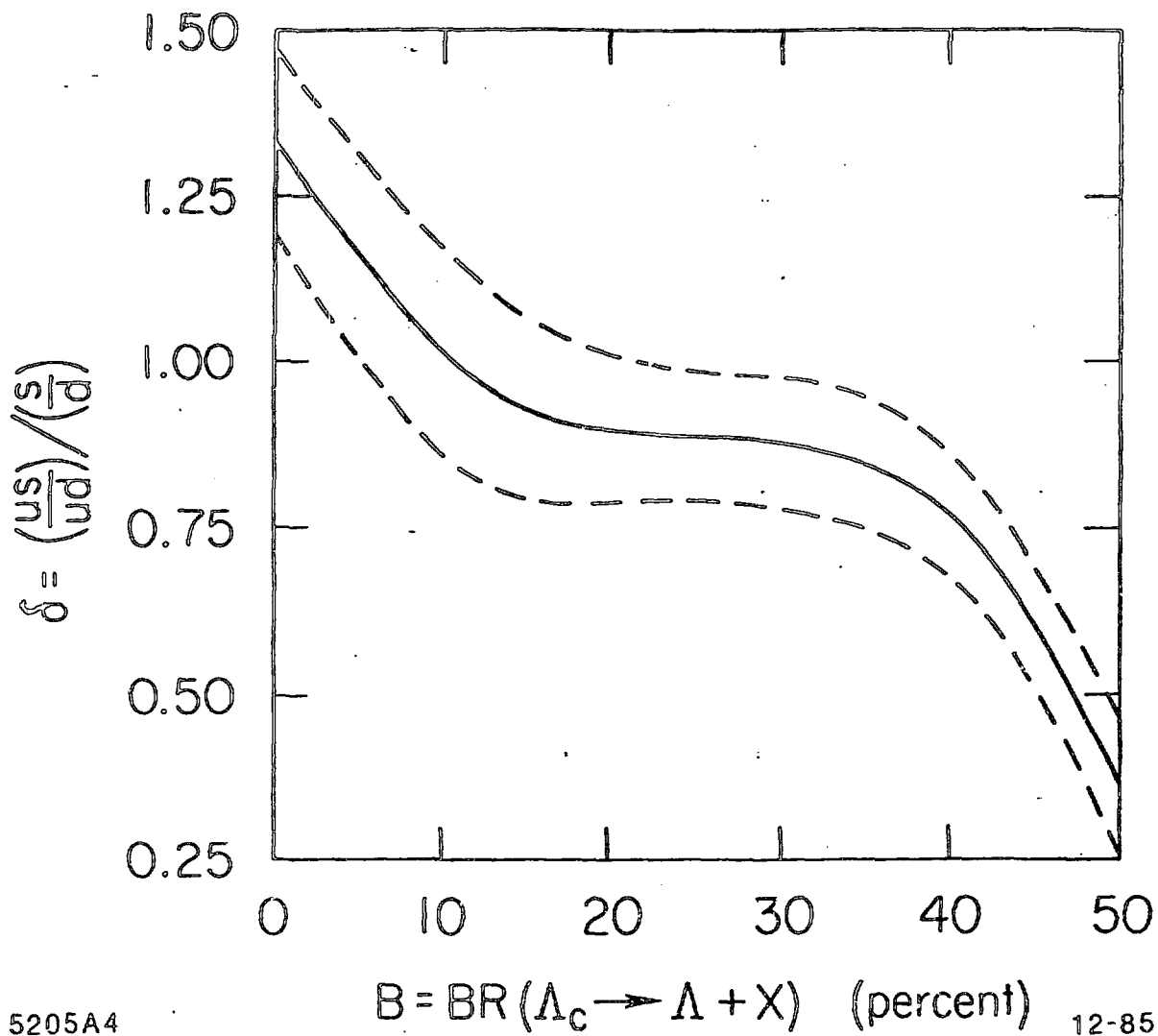


5205A3

$$y = 0.5 \ln \left[ \frac{E + p_{||}}{E - p_{||}} \right]$$

12-85

Fig. 3



5205A4

12-85

Fig. 4

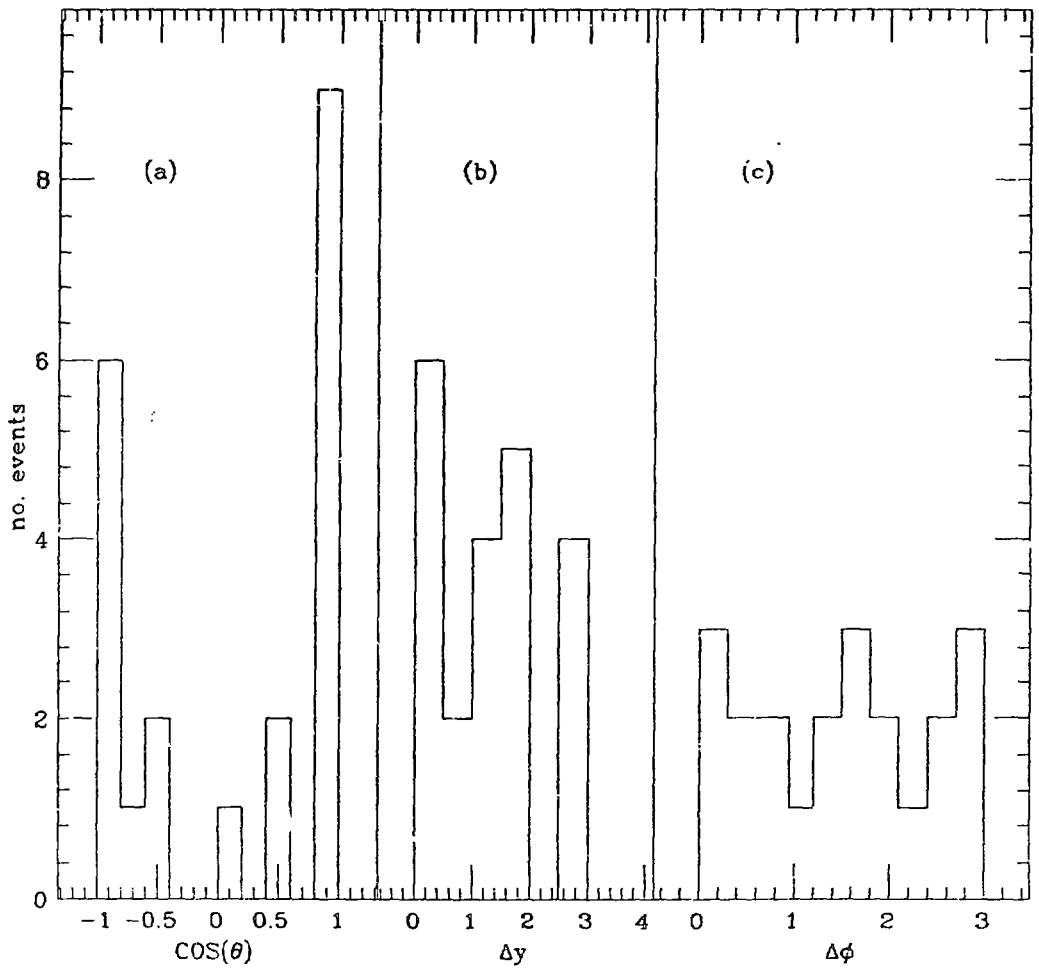


Fig. 5